Hindawi Publishing Corporation
Mathematical Problems in Engineering
Volume 2016, Article ID 7074206, 13 pages
http://dx.doi.org/10.1155/2016/7074206

Research Article

Pneumatic Adaptive Absorber: Mathematical Modelling with Experimental Verification

Grzegorz Mikułowski and Rafał Wiszowaty

Institute of Fundamental Technological Research, Ulica Pawinskiego 5B, 02-106 Warszawa, Poland

Correspondence should be addressed to Grzegorz Mikułowski; gmikulow@ippt.pan.pl

Received 15 April 2015; Accepted 30 November 2015

Academic Editor: Zhongdong Duan

Many of mechanical energy absorbers utilized in engineering structures are hydraulic dampers, since they are simple and highly efficient and have favourable volume to load capacity ratio. However, there exist fields of applications where a threat of toxic contamination with the hydraulic fluid contents must be avoided, for example, food or pharmacy industries. A solution here can be a Pneumatic Adaptive Absorber (PAA), which is characterized by a high dissipation efficiency and an inactive medium. In order to properly analyse the characteristics of a PAA, an adequate mathematical model is required. This paper proposes a concept for mathematical modelling of a PAA with experimental verification. The PAA is considered as a piston-cylinder device with a controllable valve incorporated inside the piston. The objective of this paper is to describe a thermodynamic model of a double chamber cylinder with gas migration between the inner volumes of the device. The specific situation considered here is that the process cannot be defined as polytropic, characterized by constant in time thermodynamic coefficients. Instead, the coefficients of the proposed model are updated during the analysis. The results of the experimental research reveal that the proposed mathematical model is able to accurately reflect the physical behaviour of the fabricated demonstrator of the shock absorber.

1. Introduction

Mechanical energy dissipation is an important task desired in many industry applications [1, 2]. Currently, efforts are given to increase productivity of automated plants and the speed of transportation on production lines. In parallel to increasing the transportation speed, effective means of stopping the objects on the lines are required, which is especially evident in the production processes, where the braking distance is limited due to packaging reasons [3]. The most popular technique is based on hydraulic dampers due to their effectiveness, durability, and favourable volume to force ratio [4–9]. However, in some applications the utilization of fluid-based devices is undesirable due to the possibility of toxic contamination of the goods being produced, for example, in the pharmaceutical or food industry [10, 11]. In such cases damping solutions based on pneumatics can be applied with chemically inactive gases [10, 12–14].

There are known techniques for pneumatic cylindrical shock absorbers used in aeronautical or food industries [10, 15]. However, due to the low viscosity of gases and their compressibility, the energy dissipation efficiency of these devices does not exceed 40%, while the hydraulic dampers are characterized by the efficiency of 80% [5, 15]. There exist a number of patents that propose ways to increase the effectiveness of the cylindrical pneumatic shock absorbers [16–18]. Most of the solutions are based on a double-stage algorithm of operation. After the initial compression of the gas in the cylinder, a mechanically operated valve releases the medium out of the cylinder to the surroundings. By this way the energy accumulated in the compressed gas is dissipated and the spring-back effect is diminished. These solutions increase the effectiveness of the pneumatic absorbers, but they are limited to a single, strictly defined impact energy. When the impact energy is too low, the absorber does not release the gas at the proper moment and the absorption

does not take place. Another disadvantage is related to the fact that the compressed gas is released to the surroundings, which introduces the necessity of refilling the device after each working cycle.

An improved solution considered here is based on introduction of a controlled flow between the chambers in the cylinder via the piston. In this way it is possible to dissipate energy of various magnitudes with the efficiency comparable to hydraulic devices (80%). Moreover, the gas is not released to the surroundings, which allows the device to be operated in a repeatable way. Recent developments in functional materials technology allow us to consider a novel approach to adaptive pneumatic shock absorber with utilization of a piezoelectric material for actuation of the device. A piezoelectric multilayered actuator is applied in a miniature valve positioned in the pneumatic cylinder piston [19]. In this paper we focus on mathematical modelling of the cylindrical pneumatic shock absorber with a controlled flow between the internal volumes.

Mathematical modelling of pneumatic actuators is a demanding task due to the necessity of taking into account the thermodynamic properties of the gas and the nonlinearities present in this kind of mechanical system. The nonlinearities exhibit themselves mostly due to the compressibility of the gas, internal friction, and energy transfer by heat.

Pneumatic systems are typically utilized in three domains of applications: suspensions for vibration isolation, actuation in automatics, and mechanical absorbers. Methods of the modelling are strictly related to the field of application.

Many pneumatic systems for isolation and vibration mitigation are developed for suspension of precise measuring instrumentation [20], as well as for large structures: seismic protection of buildings or large installations [21, 22]. The principle for these systems is to suspend the protected object on double chamber interconnected pneumatic springs. In these cases the devices are capable of eliminating or limiting vibrations of small amplitudes in comparison to the scale of the entire structure [23]. Since the devices can be assumed to operate in vibration of small amplitudes, several simplifications to the modelling approach can be assumed; for example, many authors investigate pneumatic systems oscillating with small amplitudes around the equilibrium position, which allows them to assume linearity of the mechanical response [24]. The second important physical phenomenon modelled in these pneumatic structures is the gas flow between the internal volumes of the structures, which has a direct influence on the dissipation properties. In many cases it is acceptable to assume a simplified model of the capillary flow based on the Poiseuille model, which is derived for viscous fluid [24]. This model assumes very low mass flow rates of the fluid, laminar flow, and low average velocity of the fluid.

In contrast to the mentioned analyses, the mathematical model of the PAA investigated in this paper must consider the state of the gas and the internal flow between the volumes enforced in the conditions of PAA under large displacements and high velocities. Such a process is nonstationary and includes large deflections of the piston and time-variant subsonic flow through the valve.

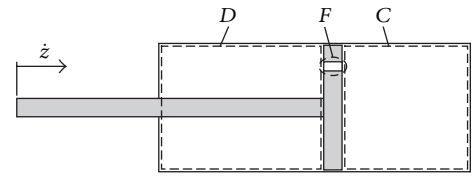

Figure 1: Schematic cross section of the considered adaptive pneumatic shock absorber.

When the pneumatic actuators are to be utilized as actuators in control of applications, the mathematical models tend to be simplified in order to find a linearised version of the plant representation, which allows the further analysis and development of a controller to be based on the classical control theory that operates most efficiently with linear, time invariant plants [25–28]. In these cases the simplification of the models is an advantage. In contrast to utilization of the pneumatic devices as actuators in automation systems, here we consider them as dampers of energy, and we need to precisely analyse the dissipation process from the point of view of its effectiveness. Therefore, a precise thermodynamic model of the structure is developed.

The thermodynamic systems are commonly described with polytropic relation and an assumption of a constant value of the polytropic coefficient. This coefficient is strongly related to the heat exchange in the system. Therefore, a constant value of the polytropic coefficient can be assumed only if the temperature of the object is stabilized, which was not the case for the considered pneumatic shock absorber.

For these reasons, in this paper we propose a numerical method for mathematical modelling of a cylindrical pneumatic dissipater with a controlled flow between internal chambers where the heat transfer, energy balance, and orifice flow are taken into account and thermodynamic state of gas is updated every calculation step.

The paper is divided into six sections, which are organised as follows. Section 2 introduces the structure of the absorber and the principle of its operation. Then in Section 3 analysis of the system is presented and a mathematical model based on thermodynamic analysis is proposed. Experimental methods and hardware are introduced in Section 4, and in Section 5 the results of an experimental verification are given before the conclusions are stated in Section 6.

2. Structure and Principle of Operation of the Adaptive Pneumatic Absorber

The conceptual pneumatic adaptive shock absorber is considered as a piston-cylinder device equipped with a fast operated valve positioned in the piston. A schematic structure of the considered device is presented in Figure 1.

In principle, the system is analysed as being able to transfer the mechanical energy of a moving body connected to the piston rod into the internal energy of the gas and then to dissipate it by heat.

2.1. The Dissipation Process. The dissipation process of the external mechanical energy by means of the absorber is conducted within three phases. The first phase is a conversion of the mechanical energy into thermodynamic energy of the gas in the process of a simultaneous expansion and contraction of the media in the two internal volumes of the absorber, C and D (Figure 1). In the subsequent phase, in order to counteract the releasing of the accumulated energy via the spring-back effect, a flow through the piston is allowed in a controlled manner, which results in a spontaneous expansion of the gas within the cylinder volumes. The effect is a decrease of the pressure difference on the piston and a limitation of the reaction force generated by the absorber. The final dissipation phase is the cooling of the gas in the cylinder by heat transfer to the surroundings. The macroscopic effect that is intended to be achieved is an elastoplastic-like response with a controllable level of plastic yielding.

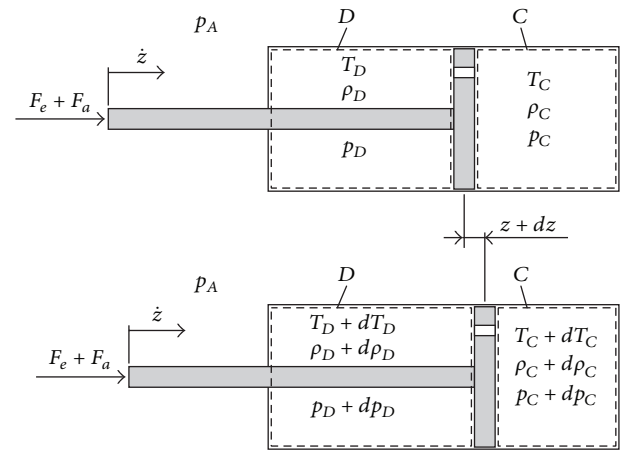

Figure 2: Scheme of the absorber.

2.2. Idea of the Control Algorithm. The adjustable gas expansion process allows the value of the reacting force to be controlled. The magnitude of the absorbed energy is adapted according to the applied algorithm. The flow process between the volumes is conducted within a period estimated as several milliseconds for the analysed range of impact velocities (up to 5 m/s). Technically it is possible to realize such a task by employing a fast operated piezoelectric valve. With this technique, it is possible to control the absorption process by adjusting the level of the mechanical energy dissipated by the system and to control the deceleration and forces acting on the protected objects.

The control algorithm for the considered dissipative adaptive system based on the absorbers can be designed to respond adequately to a wide spectrum of excitations. For the analysed conceptual, one-dimensional adaptive absorption system the process is based on three-stage operation. During the first stage, the energy of the moving object is estimated with a system of electronic noncontact sensors in a few milliseconds before the impact event. The task can be performed with a real-time system for velocity determination [29] or more advanced systems devoted to mass identification [30]. After the magnitude of the energy to be dissipated is determined, the mechanical energy of the object is converted into an increase of the enthalpy of the gas in the absorber. In the third stage, an electronically controlled process of the accumulated energy dissipation is conducted via a thermodynamically irreversible process of spontaneous gas expansion between the internal chambers of the absorber. This process was monitored and controlled by means of electronic pressure and temperature sensors positioned in the absorber cylinder. The piezoelectrically driven valve is used to adjust the process of the gas expansion and therefore to maintain the magnitude of the converted energy on a predefined level in accordance with the piston position. The algorithm is implemented in a dedicated control module that is provided with signals related to the pressures and temperatures levels in the chambers.

The presented configuration of the absorber enables us to generate the reaction force on a desired level in dependence on the magnitude of the energy to be dissipated. Therefore, the device can be considered as adaptive.

3. Mathematical Model of the Pneumatic Shock Absorber

In order to properly reflect the mechanical response of the system, it is analysed in terms of the mechanical and thermodynamic processes. The analysis is divided into three sections devoted to dynamics of the piston treated as a rigid body, thermodynamics of the gas in the absorber chambers, and gas flow through the valve. Two control volumes are distinguished inside the absorber, C and D, as depicted in Figure 2.

3.1. Forces Acting on the Piston Treated as a Rigid Body. The total force equilibrium of the piston can be defined as

$$F_e(t) - F_{p_C}(z, T_C, m_C) + F_{p_D}(z, T_D, m_D) + F_a - F_f(\dot{z}) = 0, \tag{1}$$

where the symbols are denoted as F_e, external excitation; F_{p_C}, force resulting from pressure p_C in chamber C; F_{p_D}, force resulting from pressure p_D in chamber D; F_a, force resulting from ambient pressure; F_f, friction force; z, displacement of the piston; T_C, T_D, gas temperatures in corresponding volumes; m_C, mass of the gas in volume C; m_D, mass of the gas in volume D.

The forces acting on the piston can be formulated as

$$F_{p_C} = p_C(T_C, \rho_C) \cdot A_1, \tag{2}$$

$$F_{p_D} = p_D(T_D, \rho_D) \cdot (A_1 - A_2), \tag{3}$$

$$F_a = p_a A_2, \tag{4}$$

$$F_f = f_f \operatorname{sgn}(\dot{z}), \tag{5}$$

where the following symbols are used: ρ_C, ρ_D, gas densities in chambers C and D; A_1, effective piston area; A_2, area of piston rod radial cross section; p_a, ambient pressure; f_f, friction coefficient.

3.2. Thermodynamics of the Gas in the Absorber Chambers. The thermodynamic processes in the cylinder are described with energy balance equations for the chambers: C and D, the gas state equation and the relations governing the compressible fluid flow through the applied valve. The following assumptions are introduced during the analysis.

3.2.1. Ideal Gas Law. The gas filling the volumes C and D is dry nitrogen, which is operated in the temperature above 200 K. Therefore, the assumption of the ideal gas is approved to be valid as the state of the gas is not approaching the critical point:

$$pv = RT. \tag{6}$$

3.2.2. Uniform-State, Uniform-Flow Process. Volume of the absorber chambers and the speed of sound determine the time necessary for the gas to reach the uniform state. Since the considered chambers have dimensions of the order of 0.1 m and the speed of sound in normal conditions is approximately 340 m/s, the time it takes for the gas to reach a uniform pressure is negligibly small. Furthermore, the gas is assumed to mix instantaneously in the chambers, so the fluid is described by a uniformly distributed temperature in each chamber.

The further assumptions regarding the gas dynamics are formulated as follows:

(i) the state of the mass entering the valve is constant within the time steps and uniform over the volume of the valve where the flow occurs;

(ii) the state of the mass within the control volumes can change with time, but at any instant of time the state is uniform over the entire control volume;

(iii) the changes in the kinetic energy of the gas are negligible;

(iv) the inertia and gravity forces of the gas are negligible.

3.2.3. Thermodynamic Processes Assumption. During the operation of the absorber, the gas is simultaneously compressed and decompressed in the chambers separated by the piston. The processes that take place cannot be defined clearly as isothermal or adiabatic, since the expected rate of the process varied in dependence on the work conditions. For low velocity operations the processes can be treated as close to isothermal, since in such a case there is enough time to release the energy by heat from the gas and its temperature can be assumed to remain unchanged. Otherwise, during a fast process the time is too short for the energy transfer of a significant magnitude to occur and therefore the process can be treated as adiabatic. In between the mentioned cases the process can be assumed to be polytropic:

$$pV^n = \text{const.}, \tag{7}$$

where p is pressure, V is volume, and n is polytropic coefficient. Adequately, $n = 1$ for an isothermal process and $n = 1.4$ for an adiabatic process.

In the analysed case, the model being developed is expected to reflect the behaviour of the absorber under a wide range of operational conditions and to be valid irrespective of the piston kinematics. For that reason, it is not adequate to describe the gas processes with the polytropic model with a constant parameter n.

Therefore, within each discrete time step of the computation, the state of the gas in the control volumes is calculated in the following manner: first, the gas is assumed to change its state adiabatically ($n = \kappa = 1.4$) and then the gas state parameters are recalculated based on an analysis of the internal energy balance with the heat exchange and the mass exchange between the chambers taken into account. That approach allows us to update the final state of the gas.

During each time step the following analysis is conducted:

(i) determination of the gas state change due to the volume change on the basis of the adiabatic model,

(ii) determination of the internal energy of the gas,

(iii) determination of the heat exchange between the control volume and the surroundings (with the actual area of the cylinder walls interfacing the gas computed),

(iv) determination of the energy balance in the control volume with the mass and heat exchange taken into consideration,

(v) recalculation of the gas state parameters on the basis of the energy balance equation.

This method allows us to account for the changes in the thermodynamic processes in time and therefore to reflect the polytropic-like process in dependence on the operating conditions.

The assumption of the ideal gas allows us to calculate the thermodynamic state parameters as

$$\begin{aligned} p_C(z) &= p_{C1}\left(\frac{V_{C1}}{V_{C1} - A_1 z}\right)^{\kappa}, \\ T_C(z) &= T_{C1}\left(\frac{V_{C1}}{V_{C1} - A_1 z}\right)^{\kappa-1}, \end{aligned} \tag{8}$$

where V_{C1} is the initial volume of chamber C, p_{C1} is the initial pressure in chamber C, T_{C1} is the initial temperature in chamber C, and κ is the adiabatic coefficient.

Also,

$$\begin{aligned} p_D(z) &= p_{D1}\left(\frac{V_{D1}}{V_{D1} + (A_1 - A_2) z}\right)^{\kappa}, \\ T_D(z) &= T_{D1}\left(\frac{V_{D1}}{V_{D1} + (A_1 - A_2) z}\right)^{\kappa-1}, \end{aligned} \tag{9}$$

where V_{D1} is the initial volume of chamber D, p_{D1} is the initial pressure in chamber D, and T_{D1} is the initial temperature in chamber D.

3.2.4. Mass Continuity and Energy Balance. For case of a general volume with the uniformity assumptions, the mass continuity equations for volumes C and D take, respectively, the following forms:

$$\begin{aligned} \dot{m}_C + \dot{m}_{Ce} - \dot{m}_{Ci} &= 0, \\ \dot{m}_D + \dot{m}_{De} - \dot{m}_{Di} &= 0, \end{aligned} \tag{10}$$

where m_C is the mass of the gas in the control volume C, $\dot{m}_{Ce}$ is the mass leaving the control volume C, and $\dot{m}_{Ci}$ is the mass entering the control volume C. The symbols with the subscript D denote the same quantities in volume D.

The energy balance in the control volumes can be stated as [31]

$$\begin{aligned} \dot{Q}_C + \dot{m}_{Ci} h_D &= \dot{W}_C + \dot{m}_{Ce} h_C + \frac{d}{dt}\left(m_C u_C\right), \\ \dot{Q}_D + \dot{m}_{Di} h_C &= \dot{W}_D + \dot{m}_{De} h_D + \frac{d}{dt}\left(m_D u_D\right), \end{aligned} \tag{11}$$

where $\dot{Q}_C$ is the heat transferred to the control volume C, h_C is the specific enthalpy of the gas occupying control volume C, $\dot{W}_C$ is the work done by the gas in the control volume C, and u_C is the specific internal energy of the gas in volume C. The symbols with index D describe the same quantities related to volume D.

The values of $\dot{Q}_C$ and $\dot{Q}_D$ depend on the difference between the temperatures of the gas in the respective control volume and the surroundings, the area of cylinder walls that the gas is in contact with, and the material constants,

$$\begin{aligned} \dot{Q}_C &= A_C(z) \cdot \alpha \cdot \left(T_C(t) - T_a(t)\right), \\ \dot{Q}_D &= A_D(z) \cdot \alpha \cdot \left(T_D(t) - T_a(t)\right), \end{aligned} \tag{12}$$

where $A_C(z)$ is the area of cylinder being in contact with gas in volume C, α is the heat transfer coefficient, and $T_a(t)$ is the ambient temperature. The symbols with index D describe the same quantities related to volume D.

According to the continuity principle, the mass of gas leaving the control volume C is equal to the mass of gas entering the control volume D and vice versa:

$$\dot{m}_{Ct} = -\dot{m}_{Dt}, \tag{13}$$

where

$$\dot{m}_{Ct} = \begin{cases} \dot{m}_{Ce} - \dot{m}_{Ci} > 0 & \text{when } p_C > p_D \\ \dot{m}_{Ce} - \dot{m}_{Ci} < 0 & \text{when } p_C < p_D \end{cases} \tag{14}$$

and

$$\dot{m}_{Dt} = \begin{cases} \dot{m}_{De} - \dot{m}_{Di} > 0 & \text{when } p_D > p_C \\ \dot{m}_{De} - \dot{m}_{Di} < 0 & \text{when } p_D < p_C. \end{cases} \tag{15}$$

Let us denote the transferred mass of gas as

$$\dot{m}_t = \dot{m}_{Ct} = -\dot{m}_{Dt}. \tag{16}$$

The specific enthalpies h_C and h_D of the gas in the volumes C and D, respectively, are different in general. Therefore, when the assumption of the isenthalpic flow through the valve holds true, the specific enthalpy of the gas transferred between the volumes depends on the flow direction, and it is equal to

$$\begin{aligned} h_C &= c_p T_C, \quad \text{when the gas leaves volume } C, \\ h_D &= c_p T_D, \quad \text{when the gas leaves volume } D, \end{aligned} \tag{17}$$

where c_p is the specific heat of the gas at the constant pressure.

In the considered range of temperatures between 200 K and 400 K the specific heat of the gas is assumed to be constant.

The work done by the gas is defined for the particular control volumes as

$$\begin{aligned} \dot{W}_C &= p_C(z)\, dV_C, \\ \dot{W}_D &= p_D(z)\, dV_D. \end{aligned} \tag{18}$$

3.3. Mass Flow Rate through the Valve. The valve is assumed to operate in a bistable, on-off mode. In the opened position the mass flow rate $\dot{m}_t$ (16) depends on the Mach number Ma and on the gas state parameters at the inlet of the valve p_0, T_0. In the model, the values are taken as equal to the actual values of the parameters in the control volumes as

$$\begin{aligned} p_0 &= \begin{cases} p_C & \text{when } p_C > p_D \\ p_D & \text{when } p_C < p_D, \end{cases} \\ T_0 &= \begin{cases} T_C & \text{when } T_C > T_D \\ T_D & \text{when } T_C < T_D. \end{cases} \end{aligned} \tag{19}$$

The flow is assumed to be an adiabatic process (there is no heat exchange between the gas and the walls of the valve but the mechanical losses are considered [19]). The flow losses are described with the discharge coefficient C_d treated as a characteristic design parameter of the valve [32]. In accordance with the throttled flow theory [31, 32], the flow is assumed to be choked when the Mach number Ma is close to 1. The mass flow rate of the gas exchanged between the chambers can be thus expressed in the form [19]

$$\dot{m}_t = \begin{cases} C_d \dfrac{\mathrm{Ma} A p_0 \sqrt{\kappa / R T_0}}{\left[1 + (\kappa - 1)\,\mathrm{Ma}^2/2\right]^{(\kappa+1)/2(\kappa-1)}}, & \text{if Ma} < 1 \\ C_d A p_0 \sqrt{\dfrac{\kappa}{R T_0}} \left(\dfrac{2}{\kappa + 1}\right)^{(\kappa+1)/2(\kappa-1)}, & \text{if Ma} = 1, \end{cases} \tag{20}$$

where A is the cross section of the flow duct, κ is the isentropic coefficient, and R is the gas constant.

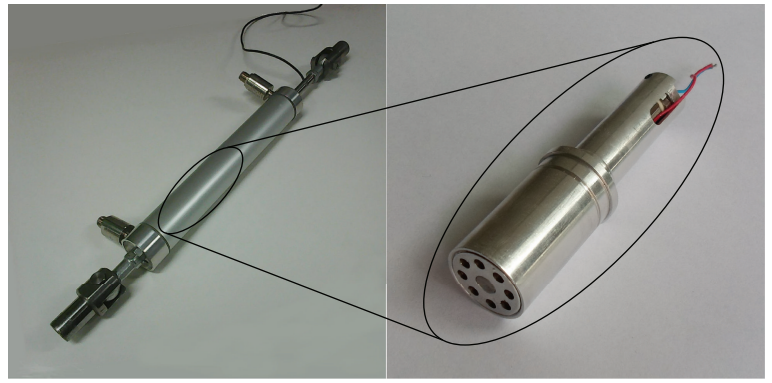

Figure 3: View of the absorber and the piezoelectric valve.

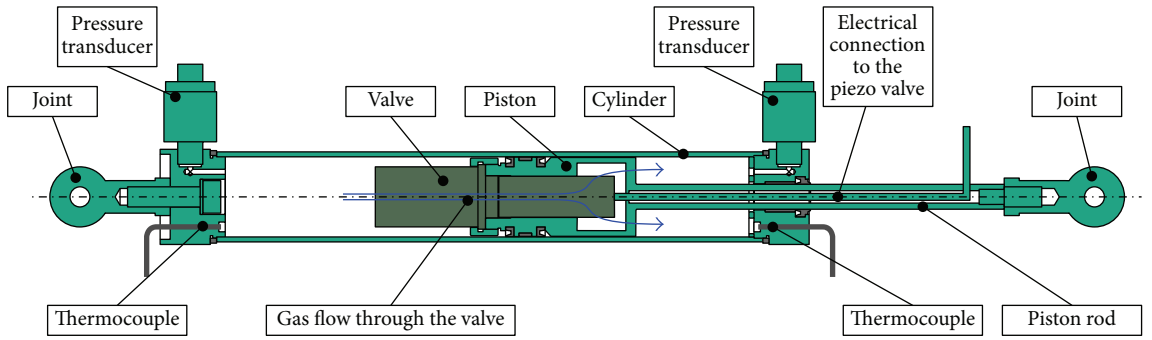

Figure 4: Main components of the absorber.

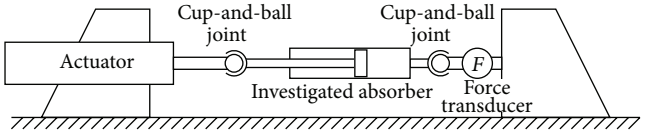

Figure 5: Scheme of the testing stand.

3.4. Governing Equations. By substituting (18) and (10) to the equations of energy balance (11), and taking into consideration (14), (15), and (17), the internal energy of the gas in the control volumes C and D can be calculated as follows:

$$\text{for } p_C > p_D$$

$$\begin{aligned} \frac{d}{dt}(mu)_C + p_C(z)\,A_1\frac{dz}{dt} + \dot{m}_t h_{tC} &= 0, \\ \frac{d}{dt}(mu)_D - p_D(z)\,(A_1 - A_2)\frac{dz}{dt} - \dot{m}_t h_{tC} &= 0, \end{aligned} \tag{21}$$

$$\text{for } p_C < p_D$$

$$\begin{aligned} \frac{d}{dt}(mu)_C + p_C(z)\,A_1\frac{dz}{dt} - \dot{m}_t h_{tD} &= 0, \\ \frac{d}{dt}(mu)_D - p_D(z)\,(A_1 - A_2)\frac{dz}{dt} + \dot{m}_t h_{tD} &= 0. \end{aligned} \tag{22}$$

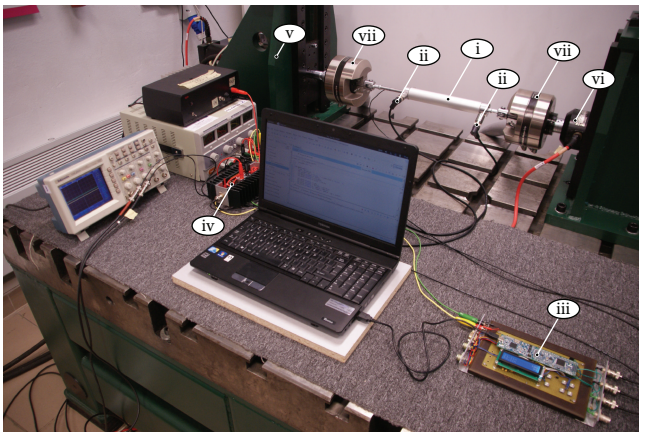

Figure 6: Laboratory testing stand.

3.5. Control Algorithm. The control procedure for the pneumatic adaptive shock absorber is aimed at maintaining a predefined level of difference between forces (2) and (3) acting on the piston. The pressure of the gas has a direct impact on the reaction force generated by the absorber. The valve opening control function has the following form:

$$C(t) = \begin{cases} C_{\text{open}}, & \text{if } F_e(t) > F_{\text{ref}} + \Delta F \\ C_{\text{close}}, & \text{if } F_e(t) < F_{\text{ref}} - \Delta F, \end{cases} \tag{23}$$

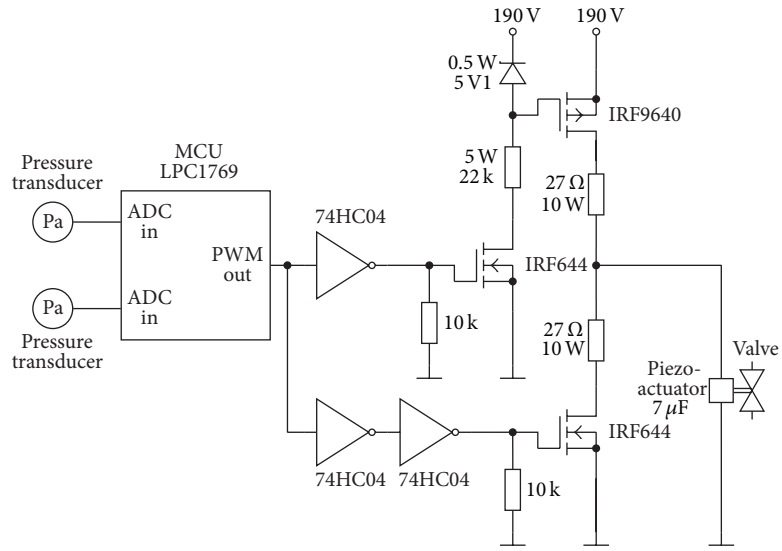

Figure 7: Scheme of the laboratory control system.

where symbols are denoted as $C_{\text{open/close}}$, signal of opening/closing the valve; $F_e(t)$, reaction force; F_{ref}, reference level; ΔF, tolerance range.

4. Experimental Program

The data required to verify the proposed method of modelling is acquired by means of a small scale device. The considered concept of the adaptive pneumatic absorber is demonstrated in laboratory scale with a demonstrator presented in Figure 3. The device is designed in dimensions: 32 mm diameter, 300 mm length, and 100 mm stroke, which allowed it to dissipate the energy of 40 J per stroke.

The demonstrator is a piston-cylinder device equipped with a valve positioned in the piston. In order to ensure the adequately short time response of the system, the valve is activated with a piezoelectric stack. The closed loop control system of the demonstrator is fed with signals from two pressure and two temperature sensors positioned within the absorber housing as depicted in Figure 4.

The testing campaign of the absorber is conducted by means of a hydraulic excitation system. The system consists of an electronically controlled servohydraulic actuator (MTS 242.01 actuator, Eden Prairie, MN, USA), positioned horizontally in line with the tested adaptive absorber (Figure 5). The actuator-absorber connections are realized via cup-and-ball joints in order to prevent the transmission of bending moments and shear forces into the structure of the tested specimen. The actuation system enables us to examine the absorber under periodic axial loading with the displacement reference signal.

The complete experimental stand is depicted in Figure 6 and consists of

(i) adaptive absorber,

(ii) pressure transducers,

(iii) electronic control unit,

(iv) piezoelectric valve supplier,

(v) hydraulic excitation system,

(vi) force cell,

(vii) hydraulic grips.

The testing program is aimed at verification of the proposed mathematical model under a variety of excitation conditions. The independent parameters are the rate of displacement, the initial pressure inside of the cylinder, and the expected (controlled) magnitude of the reaction force. The testing program is defined as follows:

(i) kinematic excitation with triangle signal, amplitude 40 mm, frequency computed based on the expected velocity of the piston,

(ii) velocity of the piston: 0.25 m/s,

(iii) initial gas pressure in the cylinder: 0.3 MPa, 0.5 MPa,

(iv) ambient pressure: 100 kPa,

(v) ambient temperature: 292 K,

(vi) magnitude of the reaction force: 100 N, 200 N, 300 N, 400 N, and 500 N.

4.1. Electronic Control Module and Control Algorithm Realization. The proposed control algorithm is realized in laboratory conditions with an intentionally designed and fabricated control system that operates in closed loop. The system consists of a microcontroller, a power supply for the piezoelectric valve, and a set of transducers (Figure 7).

The control of the reaction force in the absorber is achieved through the use of the feedback loop that is composed of

(i) control module, the circuit with the microcontroller unit (MCU),

(ii) voltage supplier,

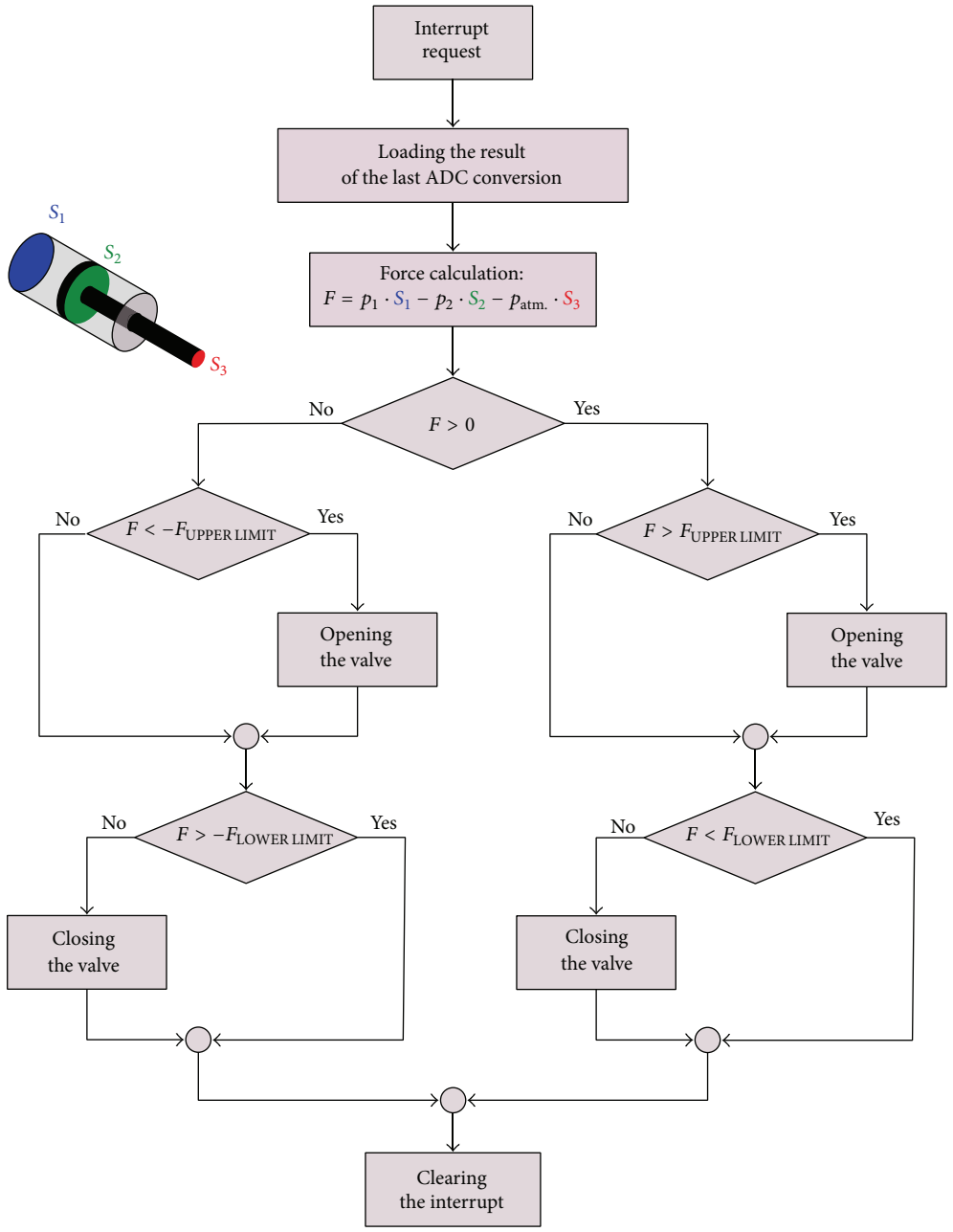

Figure 8: Algorithm executed in the interrupt service routine.

(iii) voltage relay, the circuit adjusting the driving signal according to the specific characteristics of the piezoelectric stack in the valve.

MCU peripherals include analog to digital converters (ADC) that in the assembled system are connected to the outputs of the pressure transducers. On the basis of the pressure measurements, the forces acting on the piston are computed in the MCU (denoted by LPC 1769 in Figure 7). The calculated values act as the input signals for a Pulse Width Modulation (PWM) control algorithm, which operates the valve in a bistable mode. The PWM output is amplified by means of the voltage relay and feed to the piezoelectric actuator.

The algorithm implemented in the MCU is presented in Figure 8. Every time step of operation, the following routine is executed: after the interrupt request comes from the PWM clock, the most recent ADC conversion result is stored in the variables representing pressure values inside the cylinder (see Figure 8). In the subsequent steps of the interrupt handler, the force coming from the gas acting on the piston is calculated and checked if it is positive or negative. Then it is compared to the two previously defined limits

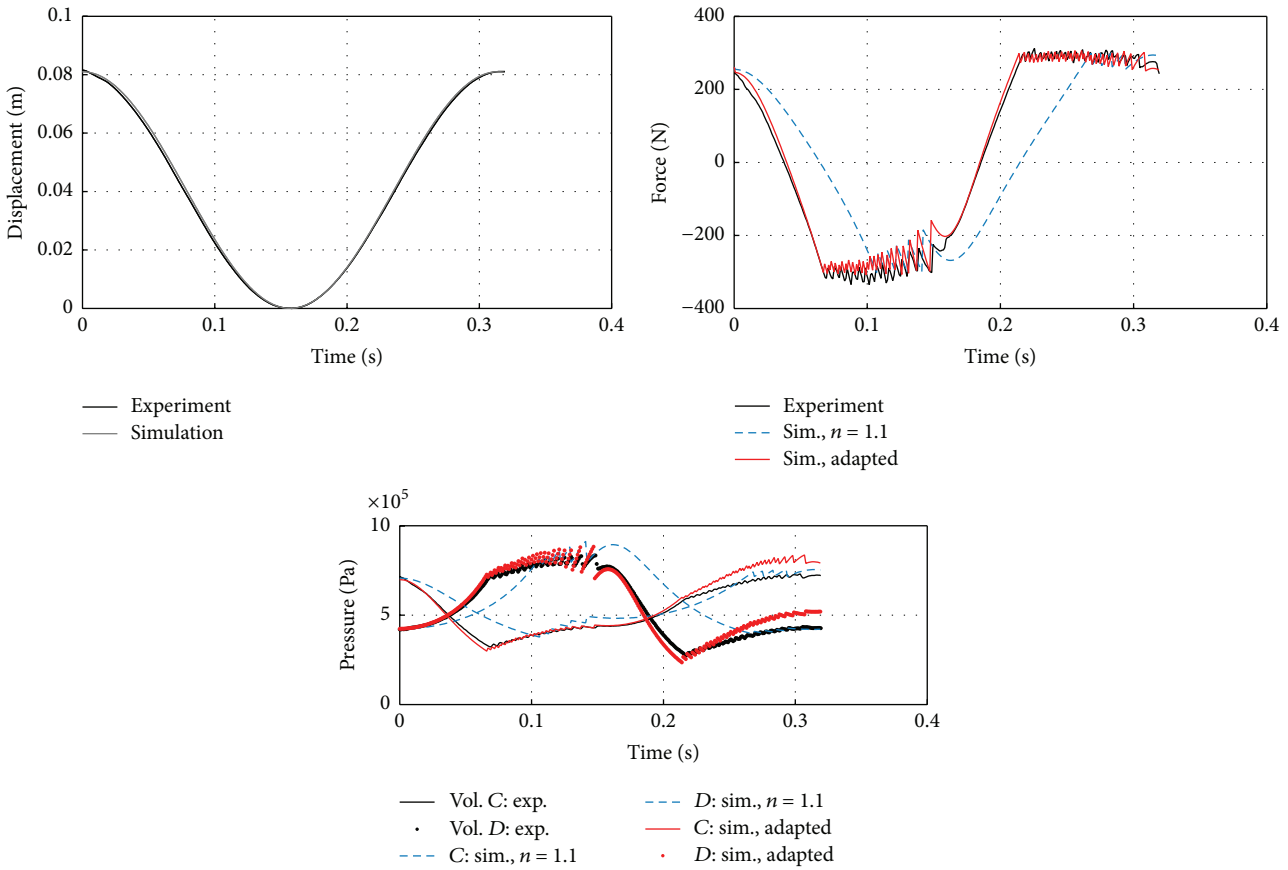

FIGURE 9: Comparison of simulation results obtained with two thermodynamic models: with a constant value of the polytropic coefficient (blue plot) and with a recalculated value of the polytropic coefficient (red plot). Excitation path (displacement) and mechanical response (reaction force and pressure) of the adaptive absorber at $p_{\text{init}} = 0.5$ MPa, CTRL = 300 N, and $f = 20$ Hz.

$F_{\text{UPPER LIMIT}}$ and $F_{\text{LOWER LIMIT}}$, which define the reference range for the desired force level.

5. Results

The data acquired during the experimental tests are compared to the results coming from the numerical simulation. The comparison is conducted for several operational conditions of the absorber in accordance with a defined testing program. The principle aim of this task is to verify the proposed mathematical model versus the experimentally obtained data. The parameters of the numerical model utilized in the example analysis are summarised in Table 1.

The conducted verification campaign has three objectives: first, to reveal the advantage of the proposed method of modelling in comparison to a model with a constant value of the polytropic coefficient; second, to exhibit a proper response of the model under various conditions of excitation; third, to prove the correct reaction of the model to a change of control input signals.

A comparison between the response of the proposed model and a one with a constant value of the polytropic coefficient is depicted in Figure 9. The presented results are obtained for a sinusoidal displacement excitation with the velocity range of 0–0.5 m/s. The conditions of the test are initial pressure in the cylinder $p_{\text{ini}} = 0.5$ MPa, control signal input CTRL = 300 N, displacement amplitude $a = 0.04$ m,

TABLE 1: Model parameters.

Piston area	A_1	8.042$e-04$	[m^2]
Piston rod area	A_2	7.854$e-05$	[m^2]
Cylinder wall thickness	d	0.002	[m]
Cylinder diameter	D	0.032	[m]
Initial volume C	$V_{C_{\text{ini}}}$	9.402$e-05$	[m^3]
Initial volume D	$V_{D_{\text{ini}}}$	1.165$e-05$	[m^3]
Adiabatic constant	κ	1.4	[—]
Gas constant	R	296.8	[J/(kg K)]
Specific heat by constant volume	c_v	743	[J/(kg K)]
Specific heat by constant pressure	c_p	1039	[J/(kg K)]
Heat transfer coefficient	α	20	[W/(m^{2}K)]
Valve discharge coefficient	C_d	0.6	[—]
Ambient pressure	p_a	100$e3$	[Pa]
Ambient temperature	T_a	292	[K]

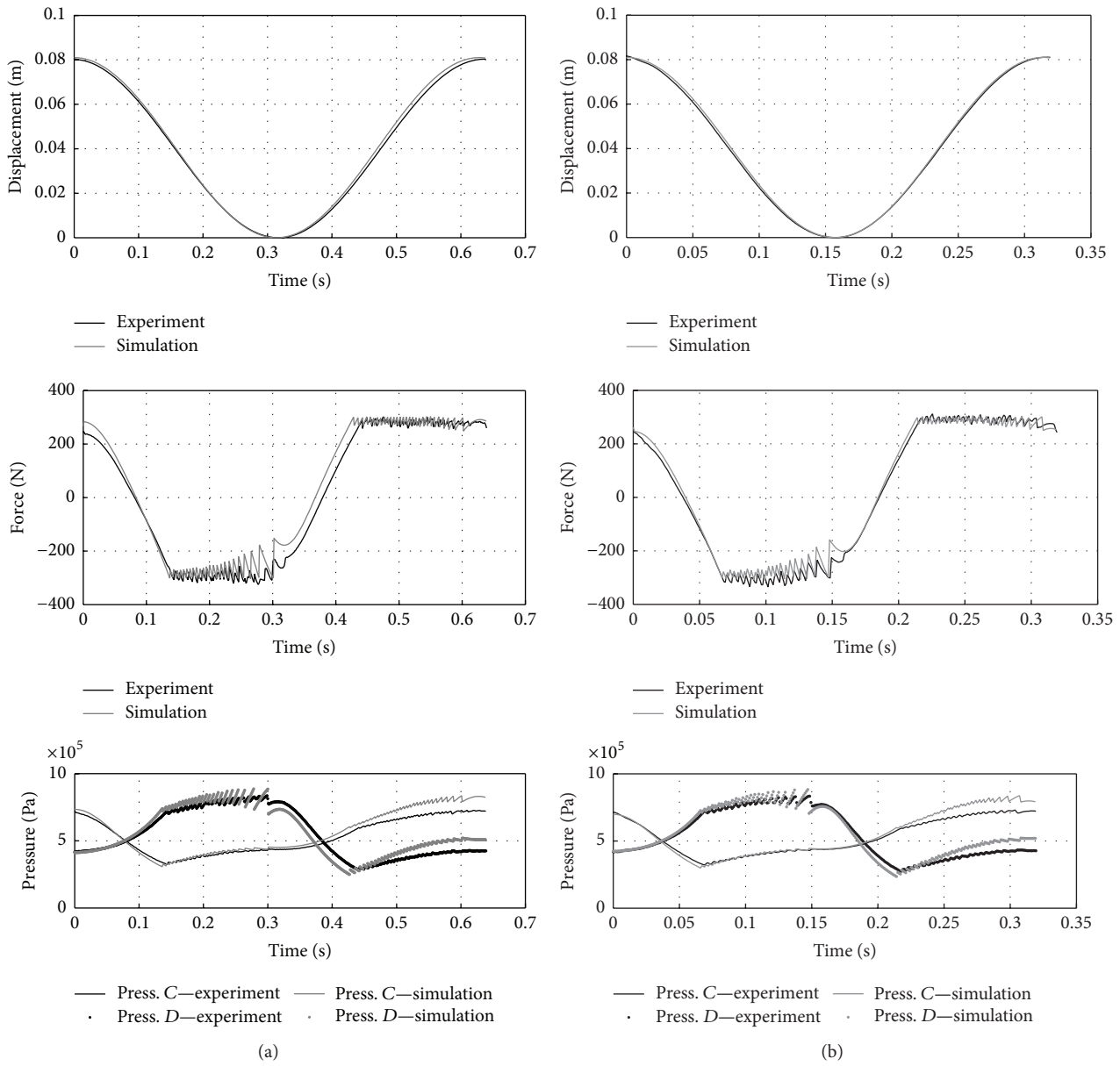

Figure 10: Verification of simulation results versus experimental data under sinusoidal excitation signal. Excitation path (displacement) and mechanical response (reaction force and pressure) of the adaptive absorber at $p_{\text{init}} = 0.5$ MPa and CTRL = 300 N. (a) $f = 10$ Hz. (b) $f = 20$ Hz.

and excitation frequency $f = 20$ Hz. The modelling results prove that the proposed model with adapted polytropic coefficient is able to reflect the absorber behaviour with a significantly increased accuracy.

The second part of the verification is devoted to proving the method of modelling the PAA under varying excitation conditions. The absorber is excited with sinusoidal signals of frequencies 10 Hz and 20 Hz and amplitude 0.04 m, which, respectively, lead to the excitation velocities 0–0.25 m/s and 0–0.5 m/s. As it is depicted in Figure 10, the proposed method of modelling allowed the mechanical response of the PAA to be reflected with minor discrepancy.

The third part of the experimental verification is aimed at proving that the proposed model is able to accommodate also a variety of control signal inputs and initial internal pressure levels. Figure 11 depicts the absorbers response in the domain of time under displacement excitation with a triangle signal. The test parameters are as follows: initial pressure: $p_{\text{ini}} = 0.3$ MPa and 0.5 MPa, excitation amplitude: $a = 0.04$ m, and control input signal: CTRL = 100 N, 200 N, 300 N, 400 N, and 500 N. Figure 12 depicts the results of verification in the domain of displacement. The presented plots reveal that the proposed model is relevant and stable in reflecting the mechanical behaviour of the PAA in the variety of conditions.

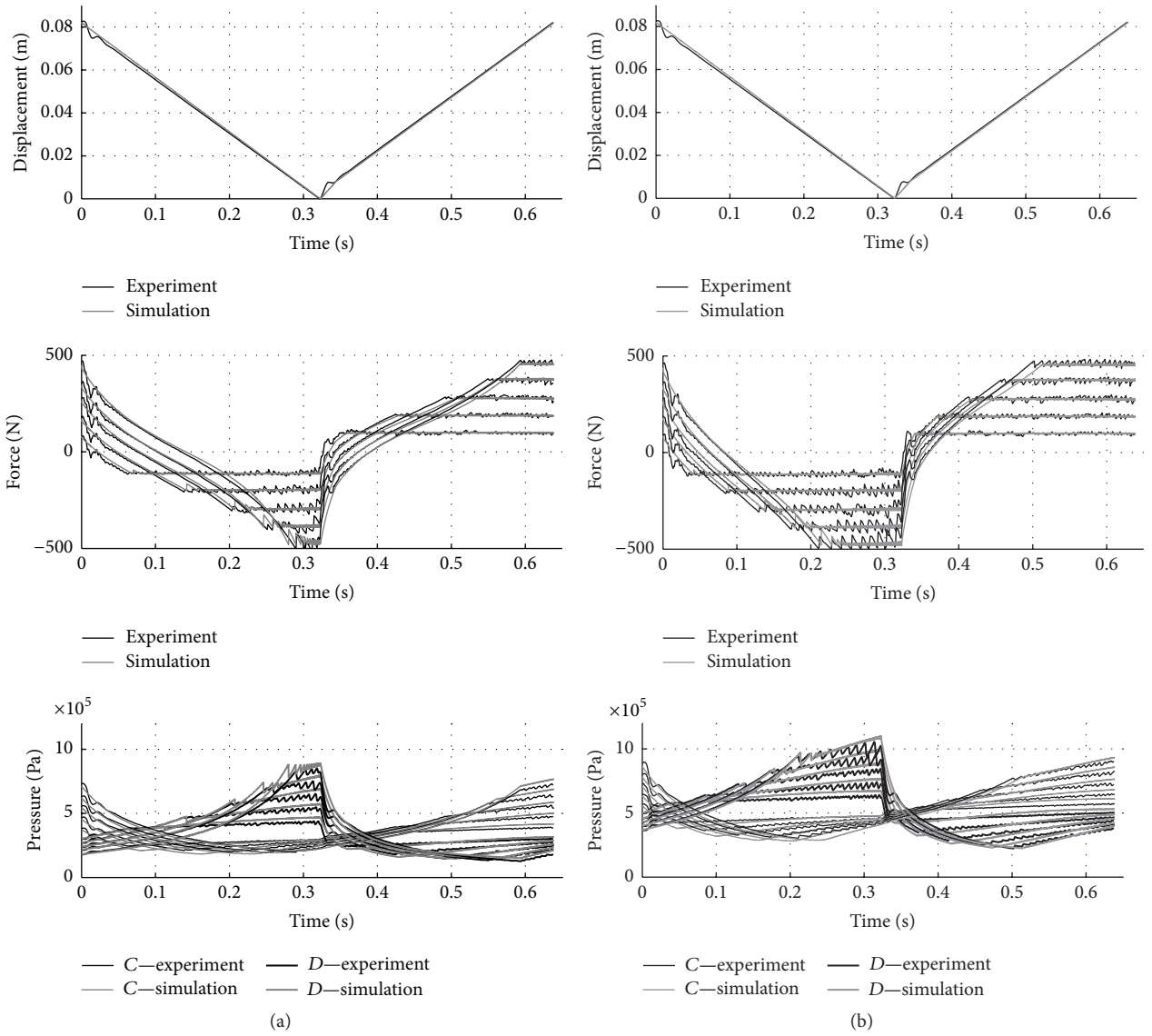

Figure 11: Verification of simulation results versus experimental data under triangle excitation signal. Excitation path (displacement) and mechanical response (reaction force and pressure) of the adaptive absorber at $v = 0.25$ m/s, CTRL = 100, 200, 300, 400, and 500 N. (a) $p_{\text{init}} = 0.3$ MPa. (b) $p_{\text{init}} = 0.5$ MPa.

6. Concluding Remarks

In this paper a method for mathematical modelling of an adaptive pneumatic absorber is presented. The absorber is a new conceptual device that might be utilized in various fields of application and therefore, from the design point of view, it is crucial to develop a reliable numerical method for reflecting its physical behaviour. The presented method of modelling with recalculation and updating of the polytropic coefficient every time step proves to be effective in reflecting the mechanical behaviour of the PAA. An advantage of the presented method is its simplicity and the relatively small demand for computation resources in comparison to the CFD methods of modelling. Therefore, it can be successfully utilized as a complementary simulation tool to the CFD approach. The model can be used for simulation of extended dynamic systems containing Pneumatic Adaptive Absorbers.

Conflict of Interests

The authors declare that there is no conflict of interests regarding the publication of this paper.

Acknowledgments

The support of Structural Funds in the Operational Programme Innovative Economy (IE OP) financed from the European Regional Development Fund Projects Modern

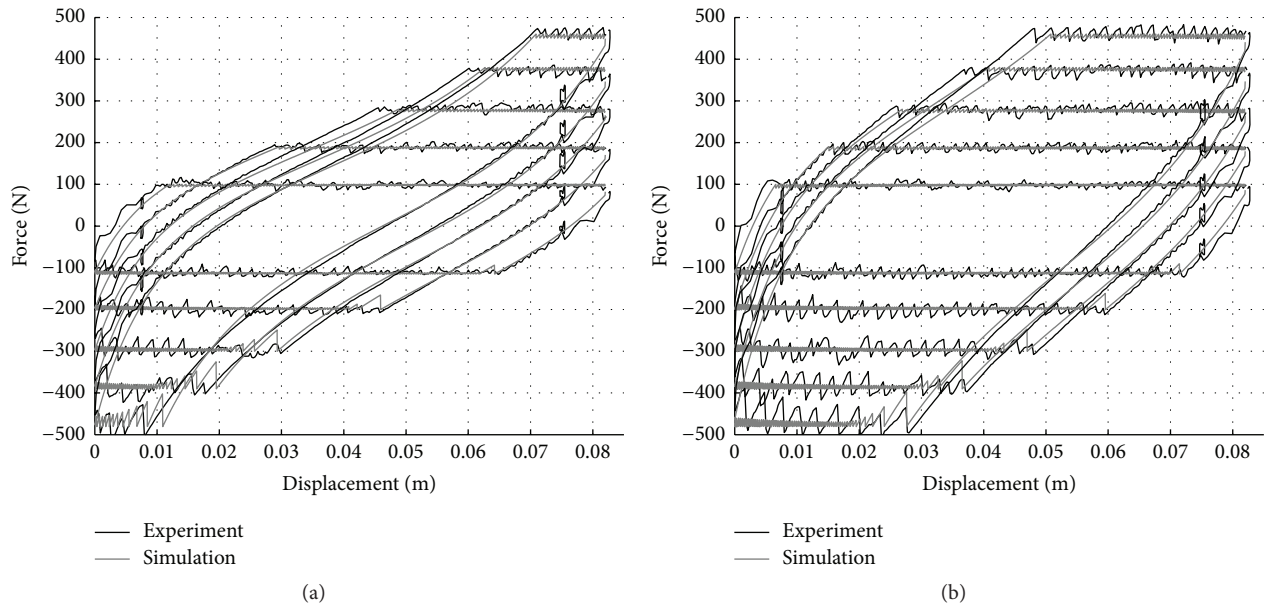

Figure 12: Verification of simulation results versus experimental data under triangle excitation signal. Reaction force of the absorber in domain of the piston displacement at $v = 0.25$ m/s, CTRL = 100, 200, 300, 400, and 500 N. (a) $p_{\text{init}} = 0.3$ MPa. (b) $p_{\text{init}} = 0.5$ MPa.

Material Technologies in Aerospace Industry (POIG.0101.02-00-015/08) and Polish National Science Centre Project AIA (DEC 2012/05/B/ST8/02971) is gratefully acknowledged.

References

[1] J. Holnicki-Szulc, C. Graczykowski, G. Mikułowski, A. Mróz, and P. Pawłowski, "Smart technologies for adaptive impact absorption," *Solid State Phenomena*, vol. 154, pp. 187–194, 2009.

[2] G. Mikulowski and R. Leletty, "Advanced landing gears for improved impact absorption," in *Proceedings of 11th the International Conference on New Actuators (ACTUATOR '08)*, pp. 363–366, Bremen, Germany, June 2008.

[3] J. Lisiecki, T. Błazejewicz, S. Kłysz, G. Gmurczyk, P. Reymer, and G. Mikułowski, "Tests of polyurethane foams with negative Poisson's ratio," *Physica Status Solidi (B)*, vol. 250, no. 10, pp. 1988–1995, 2013.

[4] C. M. Harris and A. G. Piersol, *Harris' Shock and Vibration Handbook*, McGraw-Hill, New York, NY, USA, 5th edition, 2002.

[5] Stoßdämpfer GmbH, 2015, http://www.ace-ace.com/.

[6] G. Mikułowski and Ł. Jankowski, "Adaptive landing gear: optimum control strategy and potential for improvement," *Shock and Vibration*, vol. 16, no. 2, pp. 175–194, 2009.

[7] M. Makowski and L. Knap, "Reduction of wheel force variations with magnetorheological devices," *Journal of Vibration and Control*, vol. 20, no. 10, pp. 1552–1564, 2013.

[8] P. Skalski and R. Zalewski, "Viscoplastic properties of an MR fluid in a damper," *Journal of Theoretical and Applied Mechanics*, vol. 52, no. 4, pp. 1061–1070, 2014.

[9] A. Pregowska, R. Konowrocki, and T. Szolc, "On the semi-active control method for torsional vibrations in electro-mechanical systems by means of rotary actuators with a magneto-rheological fluid," *Journal of Theoretical and Applied Mechanics*, vol. 51, no. 4, pp. 979–992, 2013.

[10] http://www.metrol.co.jp/.

[11] W. Koscielny and M. Jurczynski, "Pneumatyczne absorbery energii," *Pneumatyka*, vol. 5, no. 60, pp. 24–26, 2006.

[12] R. Zalewski and T. Szmidt, "Application of special granular Structures for semi-active damping of lateral beam vibrations," *Engineering Structures*, vol. 65, pp. 13–20, 2014.

[13] T. Szmidt and R. Zalewski, "Inertially excited beam vibrations damped by vacuum packed particles," *Smart Materials and Structures*, vol. 23, no. 10, Article ID 105026, 2014.

[14] J. M. Bajkowski, B. Dyniewicz, and C. I. Bajer, "Damping properties of a beam with vacuum-packed granular damper," *Journal of Sound and Vibration*, vol. 341, pp. 74–85, 2015.

[15] N. S. Currey, *Aircraft Landing Gear Design: Principles and Pratices*, AIAA, 1988.

[16] K. Stoll and H. Halama, "Pneumatic shock absorber," US Patent US5069317 A, 1991.

[17] A. Matsukashi, "Shock absorber," US Patent US6547045 B2, 2003.

[18] Y. Antonovsky, "High frequency shock absorber and accelerator," US Patent US6612410 B1, 2003.

[19] G. Mikułowski, R. Wiszowaty, and J. Holnicki-Szulc, "Characterization of a piezoelectric valve for an adaptive pneumatic shock absorber," *Smart Materials and Structures*, vol. 22, no. 12, Article ID 125011, 2013.

[20] J.-H. Lee and K.-J. Kim, "Modelling of nonlinear complex stiffness of dual-chamber pneumatic spring for precision vibration isolations," *Journal of Sound and Vibration*, vol. 301, no. 3–5, pp. 909–926, 2007.

[21] G. S. Aver'yanov, R. N. Khamitov, and A. V. Zubarev, "Dynamics of oscillatory systems with controllable shock absorbers," *Russian Engineering Research*, vol. 28, no. 6, pp. 543–547, 2008.

[22] C. Graczykowski and J. Holnicki-Szulc, "Protecting offshore wind turbines against ship impacts by means of adaptive inflatable structures," *Shock and Vibration*, vol. 16, no. 4, pp. 335–353, 2009.

[23] G. S. Aver'yanov, R. N. Khamitov, A. V. Zubarev, and A. A. Kozhushko, "Dynamics of controlled pneumatic shock-absorber systems for large objects," *Russian Engineering Research*, vol. 28, no. 7, pp. 640–642, 2008.

[24] C. Erin, B. Wilson, and J. Zapfe, "An improved model of a pneumatic vibration isolator: theory and experiment," *Journal of Sound and Vibration*, vol. 218, no. 1, pp. 81–101, 1998.

[25] M.-C. Shih and S.-I. Tseng, "Identification and position control of a servo pneumatic cylinder," *Control Engineering Practice*, vol. 3, no. 9, pp. 1285–1290, 1995.

[26] J. Wang, J. Pu, and P. Moore, "A practical control strategy for servo-pneumatic actuator systems," *Control Engineering Practice*, vol. 7, no. 12, pp. 1483–1488, 1999.

[27] S. C. Fok and E. K. Ong, "Position control and repeatability of a pneumatic rodless cylinder system for continuous positioning," *Robotics and Computer-Integrated Manufacturing*, vol. 15, no. 5, pp. 365–371, 1999.

[28] I. Maciejewski, L. Meyer, and T. Krzyzynski, "Modelling and multi-criteria optimisation of passive seat suspension vibro-isolating properties," *Journal of Sound and Vibration*, vol. 324, no. 3–5, pp. 520–538, 2009.

[29] K. Sekuła, C. Graczykowski, and J. Holnicki-Szulc, "On-line impact load identification," *Shock and Vibration*, vol. 20, no. 1, pp. 123–141, 2013.

[30] G. Suwała and L. Jankowski, "A model-free method for identification of mass modifications," *Structural Control & Health Monitoring*, vol. 19, no. 2, pp. 216–230, 2012.

[31] R. E. Sonntag and G. J. van Wylen, *Fundamentals of Classical Thermodynamics*, John Wiley & Sons, 1965.

[32] M. A. Boles and Y. A. Cengel, *Thermodynamics*, McGraw-Hill, 2nd edition, 1994.